IEEE Access
Multidisciplinary | Rapid Review | Open Access Journal

Received April 29, 2022, accepted June 1, 2022, date of publication June 8, 2022, date of current version June 15, 2022.

Digital Object Identifier 10.1109/ACCESS.2022.3181426

Development of Resistive-Ink Based Planar and Conformal Metasurfaces for RCS Reduction

PRIYANKA TIWARI, (Student Member, IEEE),
SURYA KUMAR PATHAK, (Senior Member, IEEE), AND VARSHA SIJU
Institute for Plasma Research, Bhat, Gandhinagar 382428, Gujarat, India
Homi Bhabha National Institute, Training School Complex, Anushaktinagar, Mumbai 400094, India

Corresponding author: Priyanka Tiwari (priyanka.tiwari@ipr.res.in)

This work was supported by the Institute for Plasma Research (IPR).

ABSTRACT This work reports design, development and characterization of both planar and conformal Metasurfaces using resistive Ink based lossy pattern printed on top of FR-4 dielectric substrate for RADAR stealth application. Different geometrical dimensions of the proposed unit cell have been optimized numerically using CST-Microwave Studio, to achieve 20 dB reflection reduction with 60% fractional bandwidth in frequency range 10.5–19.5 GHz under normal incidence with $0.12\lambda_L$ thickness (where λ_L corresponds to lower operating frequency) and 10 dB reflection reduction up to 40° oblique angle of incidence in the given frequency spectrum for both TE and TM polarized wave. An equivalent circuit analytical modelling has also been performed to understand and verify the numerical findings which are nearly in agreement. Polarization insensitive characteristics of developed surfaces is achieved using fourfold rotation symmetry of the designed unit cell. The designed absorbers are fabricated in form of planar, cylindrically bent and 90° dihedral Metasurfaces and are characterized using ABmm Vector Network Analyzer (VNA) system and free space measurement method. A thorough different experimental measurements are performed and it is found that measured characteristics are in agreement with numerical-analytical findings.

INDEX TERMS Radar absorber, Metasurface, equivalent circuit modelling, radar cross section (RCS).

I. INTRODUCTION

RADAR stealth technology requires low Radar Cross Section (RCS) of the aircraft/target to evade detection from the enemy radar. Over the years, many methods have been developed to reduce the RCS like redirecting the scattered wave through modifying the target geometry, active cancellation, Radar absorbing material (RAM) [1], [2] etc. The λ/4 Salisbury screen [3], [4] is one of the extensively used radar absorber with limitation of having narrow bandwidth absorption characteristics. One way to improve the broad bandwidth requirement is to use an additional resistive sheet, also called Jaumann Absorber [5], but at the expense of increased physical thickness and weight of the absorber. The development of Metasurface based absorber [6], [7], recently, overcomes the issues related to larger thickness, heavyweight and bulky size with larger surface mass density which was restricting the use of conventional absorber in space applications [8]–[10]. However, due to their resonating nature, they suffer from narrowband absorption performance [11]. To increase absorption bandwidth, various absorbers have been designed in past years [12]–[23]. Multi-resonating absorbers with enhanced bandwidth have been reported in [12]–[15]. These method increases the absorption bandwidth at the expense of increased unit cell size, thickness and weight.

To further enhance the bandwidth of the absorber, the Circuit Analogue (CA) absorber has been implemented where conductive pattern along with lossy element is printed periodically on the top of metal-backed dielectric substrate [16]. CA absorber based on lumped resistor as lossy element has been presented in [17]–[20]. In [17] and [18], CA absorber based on conductive pattern loaded with lumped resistor shows 10dB reflection reduction in frequency band 5.3-11.2GHz (70.07% fractional bandwidth (FBW)) with thickness $0.077\lambda_L$ and 8.2-13.4GHz (51.16 % FBW) with thickness $0.082\lambda_L$, respectively. A 20dB reflection reduction with FBW 40% and thickness $0.12\lambda_L$ have been reported in [19] and in [20], 83.4% FBW has been proposed, but measurement result has been reported only for

The associate editor coordinating the review of this manuscript and approving it for publication was Bilal Khawaja.

10dB reflection reduction. Implementing lumped resistor CA absorber is very costly because of time taking soldering process. Also, the use of lumped resistor in space-related application has reliability issues. The alternate optimum method to implement conductive pattern with lossy element is to use resistive ink [21]–[23]. CA absorber based on resistive ink where 10 dB reflection reduction in the frequency band 3-12 GHz (120% FBW) with thickness $0.08\lambda_L$ is reported in [21]. A 20 dB reflection reduction in frequency band 7.32-14.98 GHz (68.69% FBW) with thickness $0.146\lambda_L$ has been proposed in [22] but measurement results have been reported only for 10dB reflection reduction. In [23], 15 dB reflection reduction in frequency band 7 - 20 GHz (96.29% FBW) with thickness $0.116\lambda_L$ has been reported. Till date, most of the Metasurface based absorbers have been developed and characterized for 10 dB reflection reduction level and on planar surfaces.

However for RADAR industry application, it is well known that the maximum detection range of a target is directly related with the value of the RCS [1]. The detection range is reduced to 56 miles for a 10 dB RCS reduction whereas it reduces to 32 miles for a 20 dB RCS reduction as compared to 100 miles (arbitrary) for 0 dB RCS reduction [1]. Reduction in RCS value reduces the detection range which in turn reduces the reaction time allocated to enemy's radar system [1]. In most of the previous reported studies, the designs have reported for 10dB reflection reduction which is not enough for real time defence application. Only few studies reported 20 dB reflection reduction numerically but experimental validation have been reported for 10 dB reduction. In addition, in real time scenario for defence application, it is also required to study the performance of the developed devices for conformal Metasurfaces, as well. In these context, 20 dB reflection reduction with wide fractional bandwidth as well as different geometrical shapes of Metasurface become an important parameter to qualify the absorber material for real-time RADAR application. To address these requirements, first time we have designed, developed and characterized a broadband, polarization-insensitive and wide angle of incidence Metasurface Absorber (MA) based on resistive ink which exhibits 20 dB reflection reduction with $0.12\lambda_L$ thickness for FBW 60% (10.5 to 19.5 GHz). In addition, the proposed absorber is also implemented in different conformal shapes (planar, cylindrically bent and 90° dihedral surface) and its RCS reduction capabilities have been studied numerically and experimentally which have not been reported in previous studies to the best of author's knowledge. In another words, our study is innovative in terms of 20 dB reflection reduction as well as development and experimental validation of Conformal Metasurfaces for real time scenario RADAR application.

The organization of this paper is as follows: in section II, the design of the proposed absorber is presented. In section III, the structure is analytically studied using equivalent circuit (ECM) modeling and results are compared with the numerically simulated result. Absorption

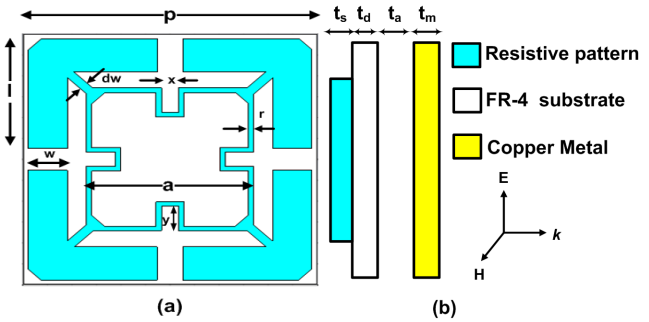

FIGURE 1. (a) Top view and (b) side view of the unit cell geometry of the proposed absorber.

characteristics of the proposed design under different polarizations of incident Electromagnetic (EM) wave and oblique incidence are studied in section IV. The losses in dielectric and metal is discussed in section V. The physics behind absorption mechanism is explained in Section VI. Extending these studies, the RCS reduction capability of the proposed absorber for planar, cylindrically bent and 90° dihedral surfaces are discussed in section VII. Fabrication process and measurement results are described in section VIII, followed by the conclusion of this paper.

II. DESIGN OF THE PROPOSED METASURFACE ABSORBER

The top and side view of the proposed Unit cell of the Metasurface absorber along with direction of the electric field, the magnetic field and propagation of the incident Electromagnetic (EM) wave have been illustrated in Fig. 1(a) and (b), respectively. Resistive patterns with surface resistance Rs = 145Ω/sq printed periodically on top of 0.2 mm thick FR-4 dielectric substrate ($\varepsilon r = 4.3$ and $\tan\delta = 0.025$). This layer is separated by a metallic ground plate using a 3.2 mm thick air spacer. Copper with thickness tm = 0.035mm and conductivity of 5.8×107 S/m has been used for ground metal plate. The optimized geometric parameters are p = 11.8 mm, a = 6.74 mm, l = 5.18 mm, w = 1.57 mm, r = 0.21mm, x = 0.68 mm, y = 1.15 mm, dw = 0.38 mm and ts = 0.01 mm. The unit cell size (p) of the proposed design is $0.413\lambda_L$ (where λ_L corresponds to the lower operating frequency of 20 dB reflection reduction bandwidth) that satisfies the subwavelength unit cell property of Metasurface.

III. EQUIVALENT CIRCUIT MODELING AND NUMERICALLY SIMULATED RESULTS

Reflection, transmission, absorption, scattering, or excitation of surface electromagnetic waves (SEWs) are the possible phenomena which takes place when an Electromagnetic wave is incident on an interface and propagate into another medium [11]. Usually, Scattering and Diffraction are dominant when surface roughness is comparable to the incidence wavelength. In Metasurfaces arrangement, dimensions of unit cell and its periodicity are small in comparison to

the centre wavelength of incident wave, we can ignore the scattering effects, particularly for planar surfaces [11]. If we consider flat surface, excitation of SEWs can be avoided because surface waves will die-out before re-scattering [11]. Transmission from the absorber can be conveniently blocked by considering metal-backed absorbing structure. Therefore, Absorptivity, A (ω), of the planar absorber under normal incidence is defined as

$$\mathrm{A}(\omega) = 1 - \Gamma(\omega) \tag{1}$$

where Γ (ω) is reflection coefficient or return loss and ω is the frequency of incident EM wave.

The proposed metasurface absorber (MA) has been modelled using a transmission line equivalent circuit model. Schematic representation of equivalent circuit model of MA is illustrated in Fig. 2(a). The top layer with resistive-ink patterns is represented as two series RLC circuit connected in parallel. Here resistance ($\boldsymbol{R_i}$) represents the losses within the resistive-ink pattern, the current path in the resistive-ink patterns is represented as inductance ($\boldsymbol{L_i}$) and the gap between two neighbouring unit cells creates the capacitance ($\boldsymbol{C_i}$), where i = 1 is for vertical resistive arms while i = 2 is for horizontal resistive arms. The FR-4 dielectric substrate is represented by a transmission line of t_d length and air spacer with the ground metal plate is represented by a short-circuited transmission line with t_a length.

From transmission line theory, the input impedance of short-circuited transmission line is defined as

$$Z_{air} = jZ_a \tan(\beta_a t_a) \tag{2}$$

where, Z_a, β_a *and* t_a are characteristic impedance, phase constant and thickness of the air spacer with the metal ground plane, respectively. Now input impedance seen from the top of FR-4 dielectric substrate represented by transmission line having length t_d can be written as

$$Z_{subs} = Z_d \frac{Z_{air} + jZ_d \tan(\beta_d t_d)}{Z_d + jZ_{air} \tan(\beta_d t_d)} \tag{3}$$

where, Z_d, β_d *and* t_d are characteristic impedance, phase constant and thickness of FR-4 dielectric substrate, respectively. Hence, input impedance at the top of MA is given by

$$Z_{in} = Z_M || Z_{subs} = \frac{Z_M Z_{subs}}{Z_M + Z_{subs}} \tag{4}$$

where, Z_M is the equivalent impedance of the top resistive patterns. The impedance of this resistive pattern is depicted by two RLC series circuits connected in parallel which can be written as

$$Z_M = (R_1 + j\omega L_1 - \frac{j}{\omega C_1}) || (R_2 + j\omega L_2 - \frac{j}{\omega C_2}) \tag{5}$$

Therefore, the reflection coefficient of the MA can be written as

$$\Gamma = \frac{Z_{in} - Z_0}{Z_{in} + Z_0} \tag{6}$$

were, Z_0 is the characteristic impedance of the free space.

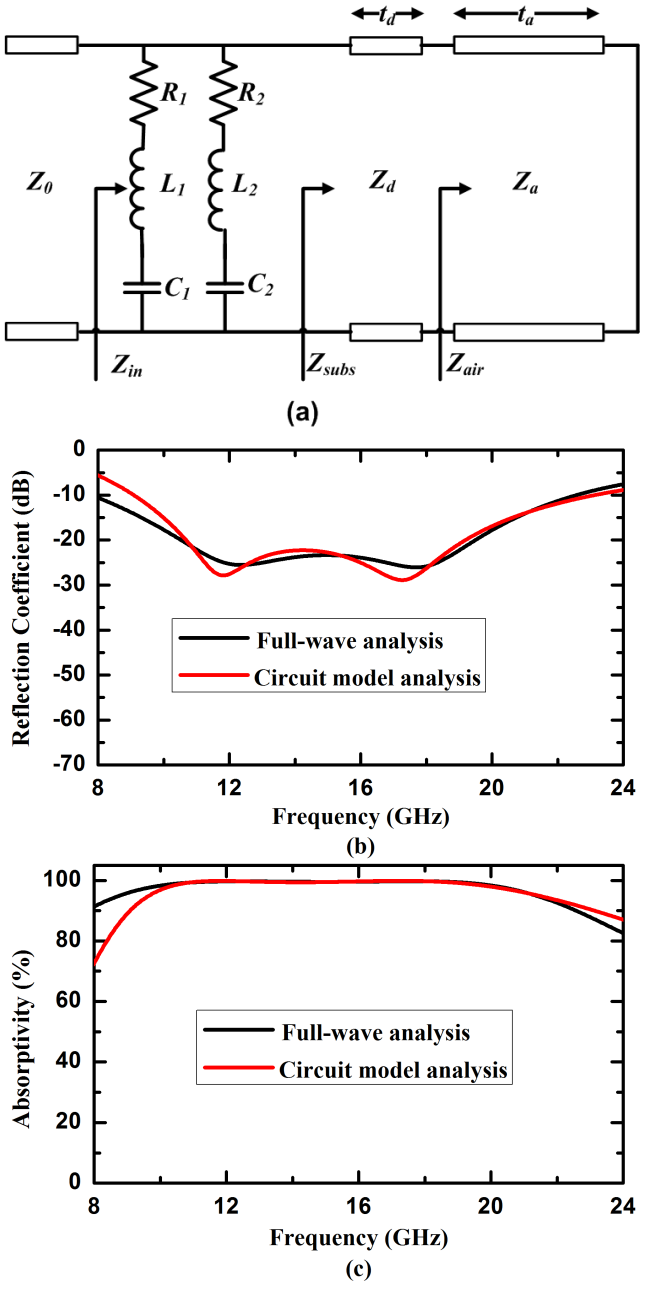

FIGURE 2. (a) Equivalent circuit model of the proposed MA, (b) Reflection Coefficient and (c) Absorptivity of the proposed MA calculated using equivalent circuit model analysis and full-wave simulation using CST MWS.

Now, the parallel circuit between the top resistive layer (with admittance Y_M) and substrate layer just below top resistive layer (with admittance Y_{subs}) resonates when Y_M have equal and opposite magnitude (in sign) with respect to Y_{subs} and which result in the purely real value of Z_{in}. Geometrical dimensions of the unit cell of the proposed MA are optimized in such a way that input impedance seen by incident EM wave (Z_{in}) has real value and matches with free space impedance (Z_o). This impedance matching will result in zero reflectivity and thus we can realize a perfect absorber.

We have used CST MICROWAVE STUDIO to design, optimize and numerically simulate the unit cell of the proposed MA keeping unit cell boundary both in x and y direction to mimic periodic patterns and open boundary condition in z-direction. We have achieved 20 dB reflection reduction (which corresponds to 99% absorptivity) from 10.5 GHz to 19.5 GHz under normal incidence. The resonance have been observed at two frequencies i.e. 12.34 GHz and 17.78 GHz. To validate the modelling of the proposed MA using the transmission line equivalent circuit model we used CST DESIGN STUDIO. With the help of curve fitting optimization analysis and reflection coefficient, which has been estimated through full-wave numerical simulation using CST MICROWAVE STUDIO, equivalent circuit parameters have been extracted and the values are as follows: $R_1 = 365\ \Omega$, $L_1 = 4.227$ nH, $C_1 = 0.03174$ pF, $R_2 = 222\ \Omega$, $L_2 = 1.0325$ nH, and $C_2 = 0.01305$ pF. Fig. 2(b) and (c) shows the reflection coefficient and absorptivity, respectively, of the proposed MA estimated using full-wave simulation by CST MWS and using equivalent circuit modelling which are in agreement with each other.

IV. CHARACTERISTICS OF THE PROPOSED MA UNDER DIFFERENT POLARIZATION AND INCIDENCE ANGLE

Characteristics of the proposed resistive ink-based MA have been studied under different polarization angle and oblique incidence to test its reliability in a real scenario and use it as a standard device.

A. VARIATION OF THE POLARIZATION ANGLE (Φ)

The unit cell of the proposed MA is designed to exhibit four-fold rotation symmetry to provide polarization-insensitive characteristics. Polarization insensitive characteristics of the proposed absorber as a function of frequency have been validated by observing its response for different angles of polarization under normal incidence. Fig. 3(a) and (b) shows the reflection coefficient and absorptivity, respectively, of the proposed resistive ink-based MA by varying angle of polarization from 0° to 90°.

B. VARIATION OF THE INCIDENCE ANGLE (θ)

Reflection coefficient and Absorption characteristics of the proposed Metasurface absorber for different angles of incidence (θ) as a function of frequency are shown in Fig. 4 (a) and (b), respectively for TE polarized incident wave. It can be seen from the figure that for TE polarized incident wave in the given frequency spectrum (10.5 GHz to 19.5 GHz), the proposed absorber maintains 10 dB reflection reduction (90% absorptivity) up to 50° of the angle of incidence. Similarly, for TM polarized incident wave, the reflection coefficient and absorption characteristics of the proposed Metasurface absorber for different angles of incidence (θ) as a function of frequency are shown in Fig. 5 (a) and (b), respectively. It can be observed from the graph that for TM polarized incident wave in the given frequency spectrum (10.5 GHz to 19.5 GHz), the proposed absorber

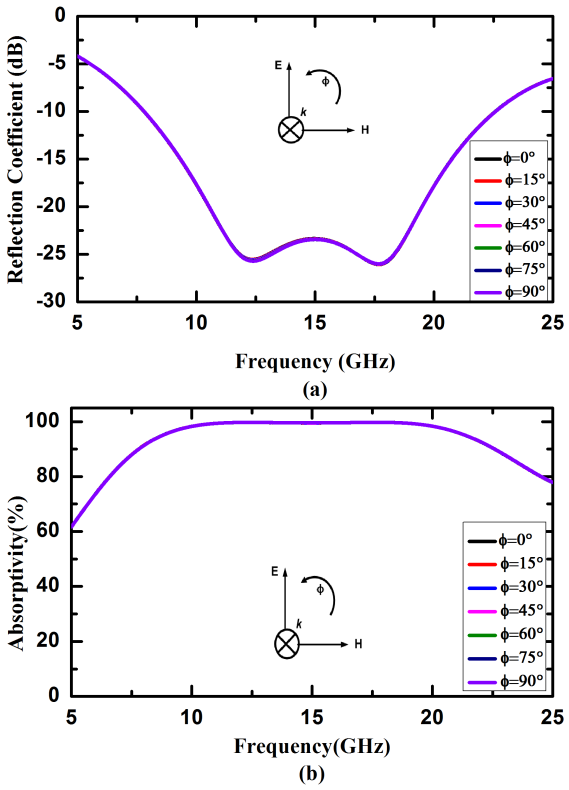

FIGURE 3. Simulated (a) reflection coefficient and (b) absorptivity of the proposed absorber for different polarization angles (Φ) under normal incidence.

maintains 10 dB reflection reduction (90% absorptivity) up to 40° of the angle of incidence. In view of these studies, the proposed Metasurface absorber can be used up to 40° of the angle of incidence for both TE and TM polarized incident wave. The performance of proposed Metasurface absorber with change in angle of incidence depends upon the electrical size of the unit cell. From the incident signal perspective, the apparent equivalent electrical size of unit cell changes with increase in incidence angle which in turn changes the reflection coefficient of absorber.

V. LOSSES IN DIELECTRIC AND METAL

In this manuscript, the concept of Circuit Analog (CA) absorber have been used, which is the extension of Salisbury screen, where a continuous resistive sheet is replaced with the geometrical patterns and which in turn gives susceptance as well as conductance, thus improves the absorption bandwidth of absorber. As the wavelength inside the absorber is a function of permittivity of the spacer, if spacer material has higher permittivity, then absorption bandwidth is reduced. Therefore, a spacer with near unity relative permittivity (air spacer) is used in between the top resistive layer and bottom metallic ground plate. The resonant frequency and admittance of the top layer is decided by geometrical shapes of these patterns and thus by optimizing these shape one can achieve the resonant frequency as per requirement. The lossy elements in the absorber are responsible to create Ohmic losses in the material when incident EM energy fall into it and thus

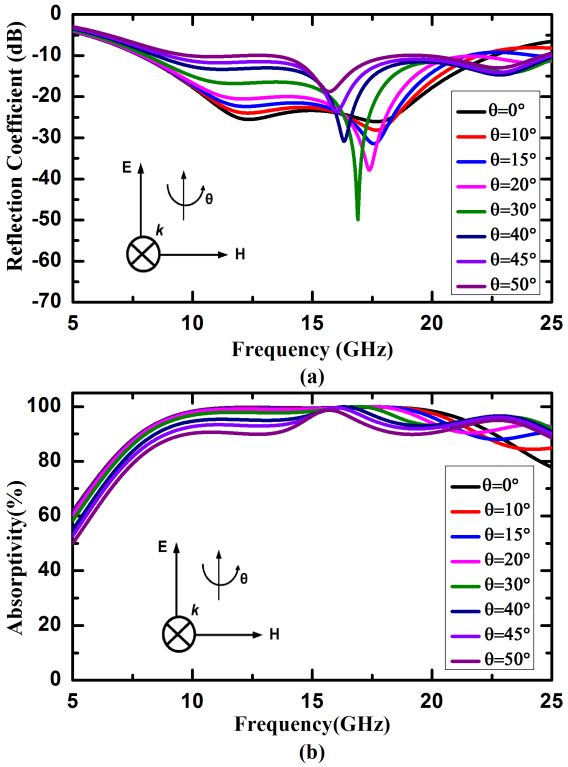

FIGURE 4. Simulated (a) reflection coefficient and (b) absorptivity of the proposed absorber for different oblique incidences (θ) under TE polarized incident wave.

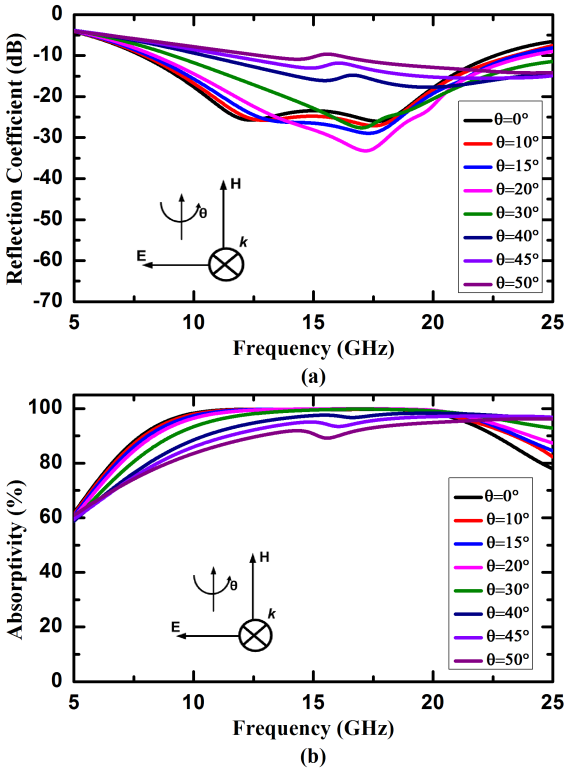

FIGURE 5. Simulated (a) reflection coefficient and (b) absorptivity of the proposed absorber for different oblique incidences (θ) under TM polarized incident wave.

get dissipated. In order to have a baseline reference and to explain the reason for implementing resistive ink concept for improvement of absorber performance, we replaced the resistive-ink pattern with metallic pattern and studied its performance. The reflection coefficient and absorptivity under normal incidence for metallic pattern and resistive-ink pattern Metasurfaces are shown in Fig 6 (a) and (b), respectively.

As shown in Fig 6 (a), the metallic pattern metasurface resonates at two frequency i.e. at 10.24 GHz and 20.38 GHz. It is also evident from Fig 6(b), that metallic pattern metasurface have less than 60% absorptivity for both the absorption band. Implementing same pattern with losses i.e. to use resistive ink pattern creates Ohmic losses in the material and thus drastically improves the performance of metasurface absorber with more than 99% absorptivity from 10.5 GHz to 19.5 GHz as shown in Fig. 6(b), keeping the resonating nature of adopted metasurface unit cell intact with little shift in resonant frequency (the resonant frequency for resistive ink pattern is 12.34 GHz and 17.78 GHz).

Power captured by absorber, dissipates either on metal or dielectric. Power dissipated in metallic part can be written as [29]

$$P_m = \frac{1}{2}\sqrt{\frac{\pi \mu f}{\sigma}} \iint_{S_m} |H|^2 \, dS \tag{7}$$

where, μ, σ and S_m is permeability, conductivity and the conductor's surface, respectively and H and f is magnetic field and frequency of the incident plane wave, respectively.

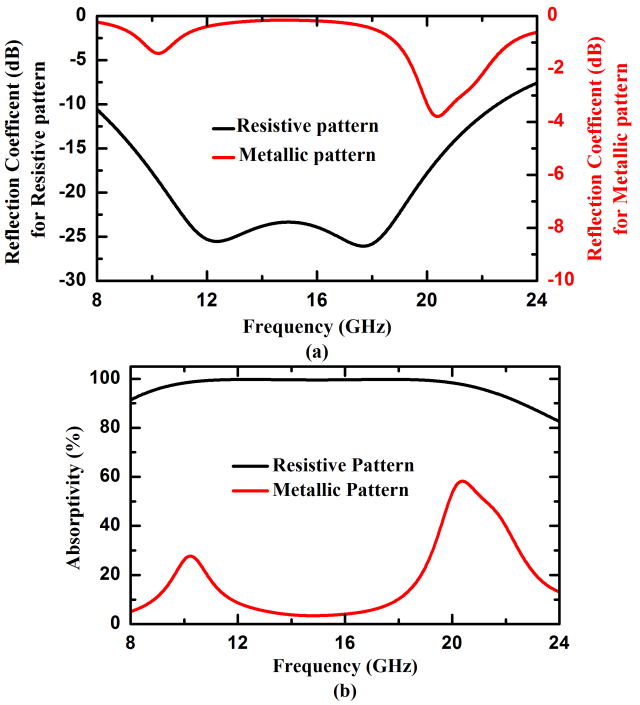

FIGURE 6. (a) The reflection coefficient and (b) absorptivity under normal incidence for metallic pattern and resistive-ink pattern Metasurfaces absorber.

Similarly, power dissipated in dielectric part can be written as [29]

$$P_d = \pi \varepsilon f \tan\delta \iiint_{V_d} |E|^2 \, dV \tag{8}$$

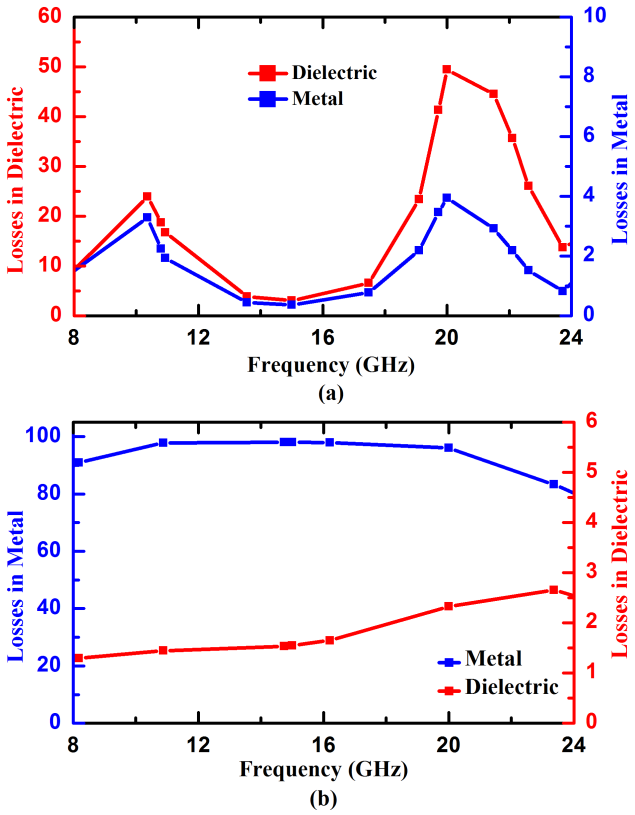

FIGURE 7. The power loss in metal and dielectric for (a) metallic pattern Metasurface absorber and (b) resistive-ink pattern Metasurfaces absorber.

where, ε, tan δ and V_d is permittivity, tangential losses, and the substrate's volume, respectively, E is electric field of the incident plane wave.

We have also calculated P_m and P_d and normalize it with total power captured by absorber for normal incidence to give the percentage of power loss in metal and dielectric, respectively. Fig. 7 (a) and (b) shows the power loss in metal and dielectric for metallic pattern Metasurface absorber and resistive-ink pattern Metasurface absorber, respectively. From Fig. 7 (a), it is clearly evident that the losses in dielectric is around 50% while the losses in metal is less than 9% for metallic pattern Metasurface absorber and therefore, dielectric loss dominating factor in this case. Whereas for resistive-ink pattern Metasurface absorber, losses in dielectric is less than 3% while the losses in metal is around 90% to 100 % and dominating factor in this case as shown in Fig 7 (b).

VI. EXPLANATION OF ABSORPTION MECHANISM USING SURFACE CURRENTS

To understand the physics behind the absorption mechanism, we observed the interaction between exciting wave and Metasurface absorber which generates equivalent electric and magnetic responses. As the unit cell size is very small as compared to the incident wavelength in the targeted frequency band, only dipolar electric and magnetic resonances will be generated in the structure and higher-order multipolar resonances will not occur [16]. Therefore the proposed Metasurface absorber can be illustrated as an equivalent array of the electric and the magnetic dipole moments. Absorption of the structure can be controlled by combining the fields scattered by the electric and magnetic dipolar resonances together. For a symmetric unit cell, the absorbing structure can be analyzed using even/odd mode analysis. When the EM wave incident on the structure and the induced surface currents are equal and opposite on top and bottom layers, then an odd mode resonance is generated which corresponds to an equivalent magnetic dipole moment. Similarly, when the induced surface currents on top and bottom layers are in the same direction, then an even mode resonance is generated which corresponds to an equivalent electric dipole moment. Induced surface current on the top resistive patch and the bottom metallic plate have been analyzed at two resonant frequencies i.e. 12.34 GHz and 17.78 GHz, to explain the absorption mechanism of the proposed absorber. Fig 8 (a) and (b) shows surface currents for TE-and TM-mode, respectively at 12.34 GHz. As we can see from the figure that for both TE and TM mode, surface current at top resistive layer and bottom metallic ground plane are antiparallel to each other that generates a magnetic field which then couples with the magnetic field of the incident EM wave and result in absorption at this frequency. Similarly, Fig. 8 (c) and (d) illustrates the surface currents at 17.78 GHz for TE-and TM-modes, respectively. It can be seen from the figure that surface current at the top and bottom of the proposed unit cell are parallel to each other and generates electric resonance in the structure, which results in absorption at this frequency.

VII. RCS ANALYSIS OF THE PROPOSED METASURFACE ABSORBER

The effective area seen by the radar contributing to radar cross-section (RCS), σ, of the target [1] and defined as the ratio of reflected power from target per unit solid angle to the incident power as given in (9).

$$\sigma = 4\pi \lim_{R\to\infty} R^2 \frac{|E_s|^2}{|E_i|^2} = 4\pi \lim_{R\to\infty} R^2 \frac{|H_s|^2}{|H_i|^2} \tag{9}$$

where 'E_s' and 'E_i' are scattered and incident electric field intensity, 'H_s' and 'H_i' are scattered and incident magnetic field intensity and 'R' is the distance from target to the receiving antenna. RCS is the measure of the detectability of the target from incoming radar and therefore, it is very important to reduce it in stealth technology. The potential targets in military application like missiles, aircraft and rockets must have low RCS so that they cannot be detected by enemy radar and thereby improving their surveillance capabilities.

A different approach to reduce RCS of the planar surface has been reported in [25] and [26], but both designs are sensitive to the polarization of the incident EM wave. A polarization-insensitive RCS reduction which is based on Polarization Convertor Metasurface (PCM) is presented in [27], but RCS analysis is reported only for planar surface. Recently, RCS reduction capability of a resistive-ink based

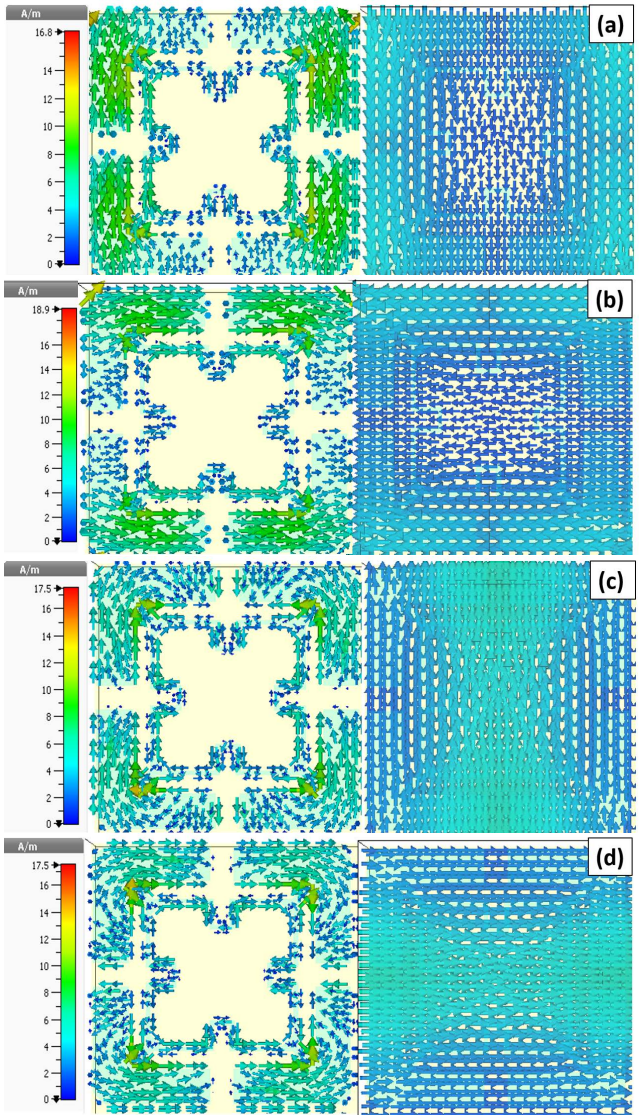

FIGURE 8. Induced surface current distribution on the top resistive and bottom metallic layer of the unit cell of the proposed MA for (a) TE and (b) TM mode at 12.34 GHz and for (c) TE and (d) TM mode at 17.78 GHz.

Metasurface Absorber has been presented in [28], but experimental validation has been reported only for planar surface. In addition, the power losses in metal and dielectric and oblique incidence characteristics for TM mode is not discussed in [28]. In order to use the proposed Metasurface absorber (MA) in real-time stealth applications, it is important to do its RCS analysis on planar, cylindrically bent and 90° dihedral surface, because these contributes most to the RCS of the target. RCS of the proposed MA is compared with the same size and shape of a Perfect Electric Conductor (PEC).

A. RCS OF MA ON PLANAR SURFACE

First, we calculated the RCS of MA on a planar surface which has 18 × 18 unit cells and compared it with RCS of the same size PEC. Fig 9(a) and (b) demonstrate 3D views of planar PEC and planar MA, respectively. For normally incident EM

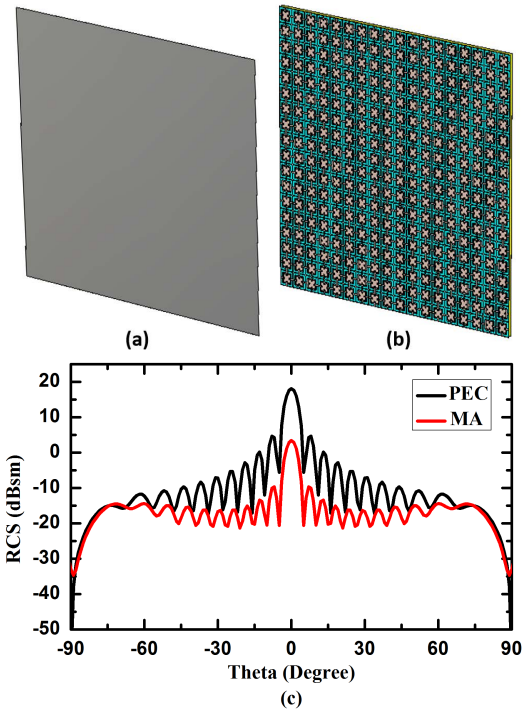

FIGURE 9. 3D view of (a) planar PEC and (b) planar MA and (c) 2D scattering patterns of PEC and planar MA at 15.20 GHz.

wave, Fig. 9(c) shows the RCS of planar PEC and planar MA at 15.20 GHz. It can be seen from the figure that the RCS of the proposed MA is significantly reduced as compared to RCS of PEC.

B. RCS OF MA ON CYLINDRICALLY BENT SURFACE

Further extending our studies, we studied the RCS reduction capability of the proposed MA on a cylindrically bent surface with 18 × 18 unit cells. 3D views of cylindrically bent PEC and cylindrically bent MA with a radius of curvature of 100mm are shown in Fig. 10(a) and (b), respectively. Fig. 10 (c) and (d) shows RCS of cylindrically bent PEC and cylindrically bent MA for radius of curvature 100mm and 50mm, respectively, for normally incident EM wave at 15.20 GHz. From Fig10 (c) and (d) it is evident that there is a significant reduction in RCS value of cylindrically bent MA as compared to cylindrically bent PEC for both the radii of curvature. From figure it is also observed that as the radius of curvature is reduced from 100 mm to 50 mm, the performance of MA on cylindrically bent surfaces in terms of RCS reduction value deteriorates.

C. RCS OF MA ON 90° DIHEDRAL SURFACE

In the third case study, we analyzed the RCS reduction capability of the proposed MA on a 90° dihedral surface with 18 × 18 unit cells on both sides and compared it with PEC. Fig 11(a) and (b) illustrate 3D views of 90° dihedral PEC and MA surface. RCS of 90° dihedral PEC and MA for normally incident EM wave at 15.20 GHz is shown in Fig. 11(c). From the figure, it is observed that the RCS of MA for 90°

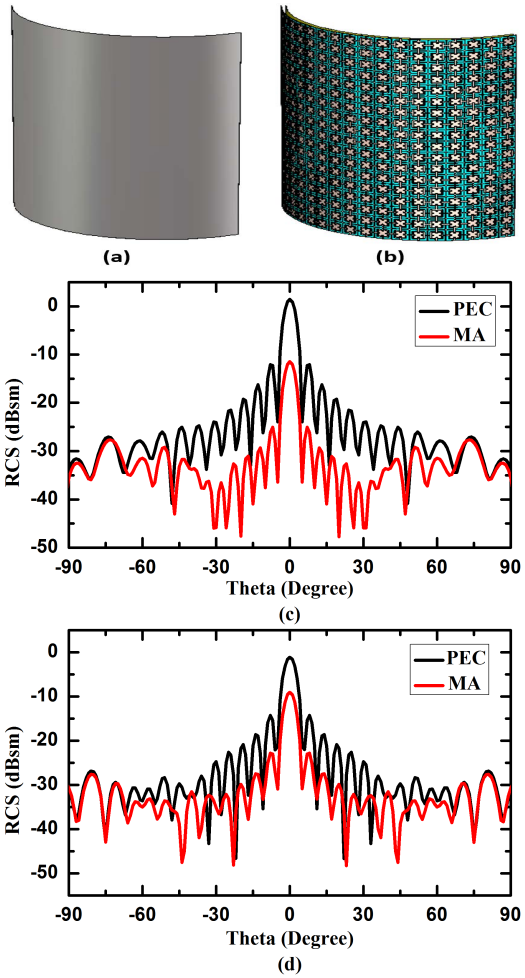

FIGURE 10. 3D views of (a) cylindrically bent PEC (b) cylindrically bent MA and 2D scattering patterns of cylindrically bent PEC and MA for radius of curvature (c) r = 100mm and (d) r = 50mm at 15.20 GHz.

dihedral surface is significantly reduced as compared to PEC. Therefore, from these observations, it can be inferred that the proposed resistive ink-based MA can efficiently reduce RCS and can be used in RADAR stealth technology.

VIII. FABRICATION PROCESS AND MEASUREMENT RESULTS

A. REFLECTION REDUCTION CHARACTERISTICS OF DEVELOPED PLANAR METASURFACE

A planar prototype Metasurface Absorber (MA) with 18 × 18 unit cells (212.4mm × 212.4mm surface area) has been fabricated to experimentally test the reflection reduction capability to qualify as RCS reduction device. YShield HSF-54 [29] ink has been used to print resistive patterns on top of 0.2mm thick FR-4 dielectric substrate with the help of screen printing technique [30]. In the screen printing technique, the first step is to develop a stencil, which is fixed in a rigid frame. This stencil is prepared by blocking the area of screen that corresponds to negative of designed pattern while opening the area from where the ink (YShield HSF-54) needs to be deposited on top of substrate. In next step, the developed stencil is properly aligned with the FR-

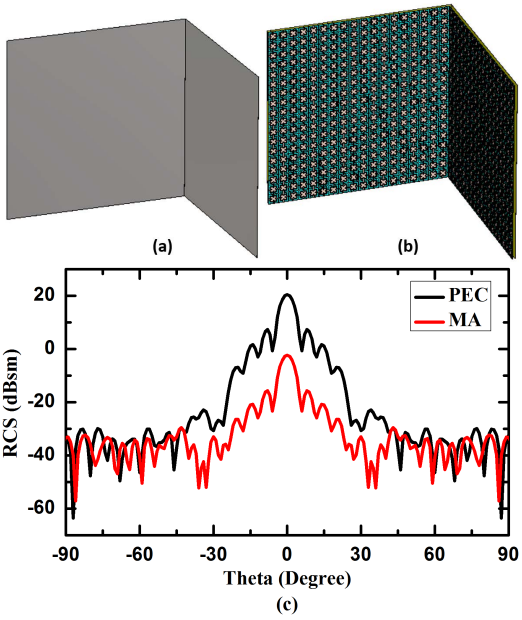

FIGURE 11. 3D views of (a) 90° dihedral PEC (b) 90° dihedral MA and (c) 2D scattering patterns of 90° dihedral PEC and MA at 15.20 GHz.

4 dielectric substrate and a squeegee is moved across the screen to fill the open mesh apertures of screen with ink and enables the deposition of the resistive ink patterns on top of FR-4 dielectric substrate. NanoMap 500ES Profilometer has been used to further confirms the thickness of printed resistive patterns which is 0.01 mm. This FR-4 dielectric layer and bottom ground metallic plate, made of copper, have been separated by Teflon screws with a spacer thickness of 3.2mm.

Fig. 12 (a) and (b) shows the 3D view of the fabricated sample and experimental set up, respectively, where ABmm Vector Network Analyzer (VNA) 8-220GHz and two linearly polarized standard gain horn antennae in two frequency sweep (8-18 GHz and 18–24GHz) have been used for measuring reflection reduction from the developed device. The fabricated sample is kept at a distance satisfying far-field requirement and Anechoic Chamber Standards. One horn antenna is used to transmit the signal while the other antenna is used to receive the reflected signal. Reflections from equal size copper metal plate have been measured and used for the calibration. For normal incidence wave, where both the transmitter and receiving antenna are collocated, measured and simulated reflection reduction of the developed device have been shown in Fig. 13(a). Reflection reduction characteristics of the developed device have also been tested under oblique angle of incidence. Figs. 13 (b), (c), (d) and (e) shows the measured and simulated reflection reduction characteristics as a function of frequency (specular measurement) for 10°, 20°, 30° and 40° angle of incidence, respectively. It is observed from the figures that measured reflection reduction under normal incidence and oblique incidence has a very good match with simulated results. From the graph one can see that reflection reduction characteristic of the developed device exhibits wide angle of incidence.

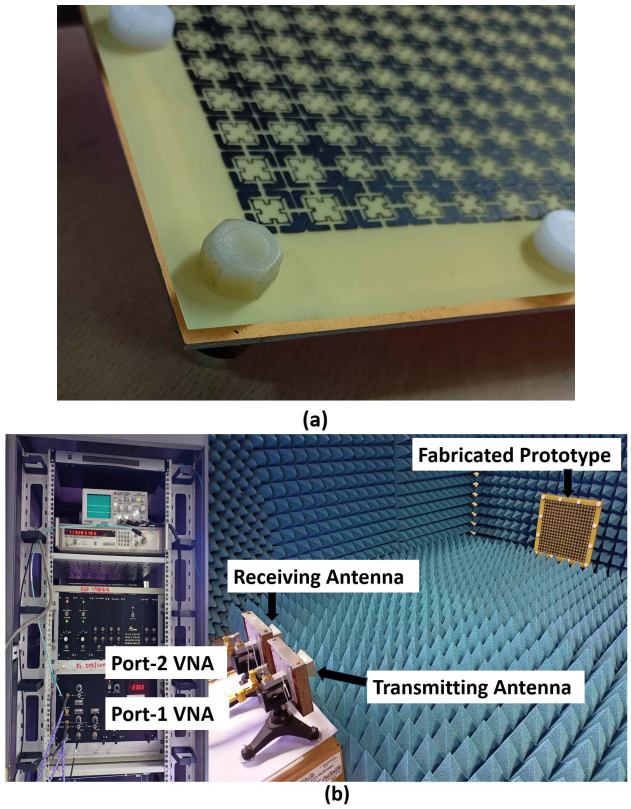

FIGURE 12. (a) 3D view of the fabricated sample and (b) Experimental setup.

B. REFLECTION REDUCTION CHARACTERISTICS OF DEVELOPED CONFORMAL METASURFACES

In real-time scenario, the RADAR target will be wrapped with different geometrical shapes of the Metasurfaces. Therefore, it is mandatory to qualify the Reflection Reduction characteristics of conformal Metasurfaces for RCS application. The developed planar Metasurface has been now reconfigured in cylindrically bent and 90° dihedral surfaces.

For cylindrical surface planar Metasurface is bent in cylindrically bent surface with radius of curvature 200mm. Here, we have used very thin bottom metallic layer (with 0.2 mm thickness) so that it conveniently bend around the surface. Fig 14 (a) depicts the developed cylindrically bent Metasurface and the experimental setup for its characterization while Fig 14 (b) exhibits the simulated and measured reflection reduction under normal incidence (both transmitter and receiver antenna kept at 0° with respect to normal to surface) for cylindrically bent Metasurface with radius of curvature 200mm. It is evident from the figure that measured result matches well with numerically simulated result for the same 20 dB reflection reduction bandwidth.

Due to curvature in the surface, some power will be scattered in the direction other than backward direction and therefore it is required to measure the scattering power at other angles, as well. To measure scattered power transmitter antenna has been fixed at 0° (with respect to normal to surface) and receiver antenna is scanned from 10° to 40° (with

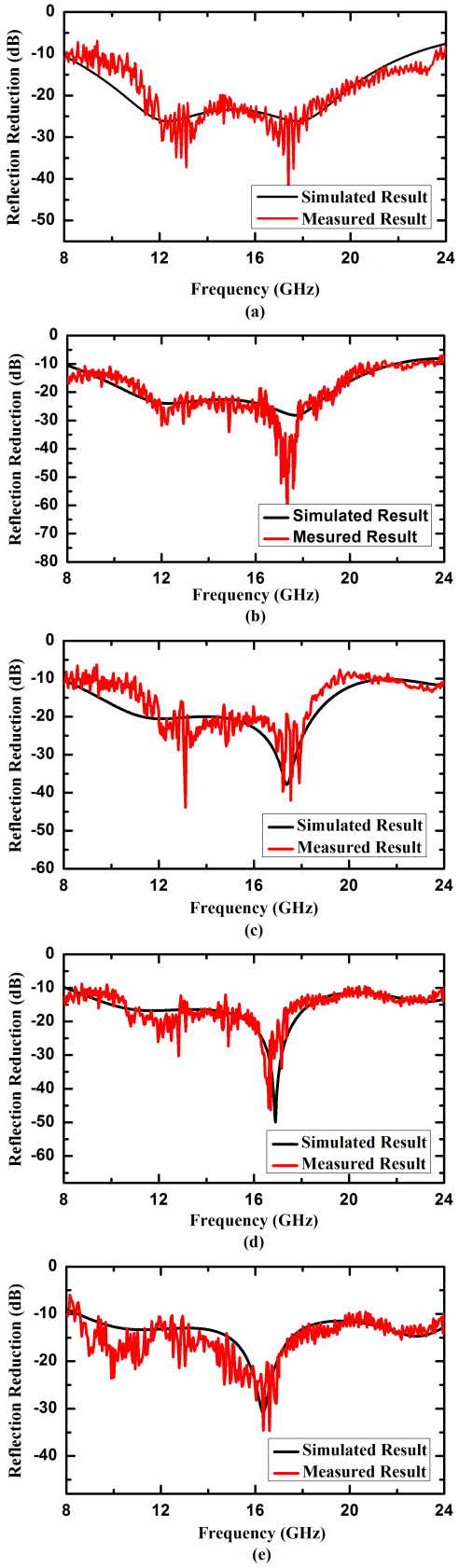

FIGURE 13. Simulated and measured reflection reduction characteristic of the developed planar Metasurface absorber under (a) normal incidence, (b) 10°, (c) 20°, (d) 30° and (e) 40° angle of incidence (specular measurement).

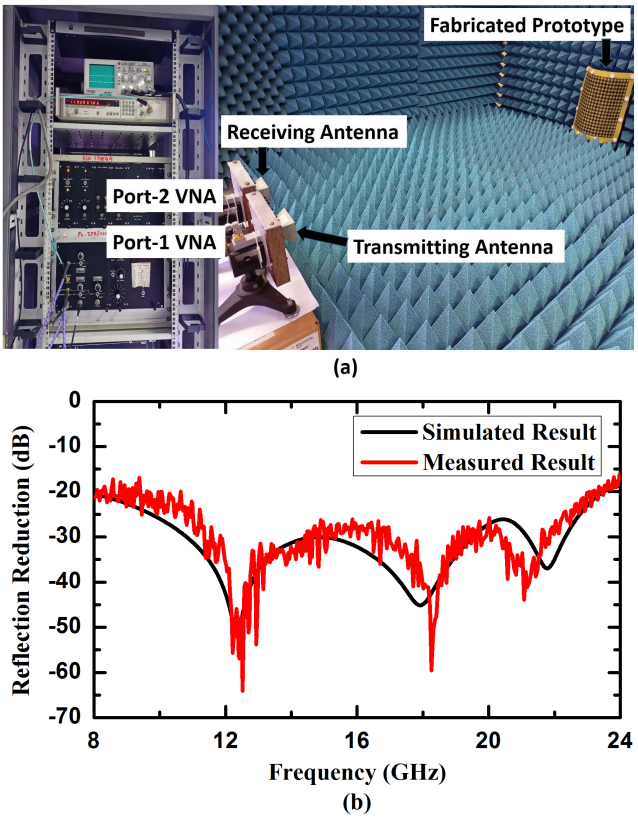

FIGURE 14. (a) Experimental setup and (b) The simulated and measured reflection reduction under normal incidence for cylindrically bent Metasurface with radius of curvature 200mm.

respect to normal to surface) on either side. Measured result for scattered power under normal incidence have been shown in Fig 15.

Similarly, reflection reduction measurement under normal incidence for 90° dihedral Metasurface has been performed. In this configuration, Fig 16 (a) depicts the experimental setup and Fig 16 (b) shows the simulated and measured reflection reduction values under normal incidence. The measured results are in good agreement with numerically simulated result.

IX. A COMPARATIVE PERFORMANCE OF THE DEVELOPED DEVICE WITH PREVIOUS REPORTED WORK

Table 1 presents a comparative study of reflection reduction characteristics and RCS reduction capability of the developed Metasurfaces with previously reported studies. It can be seen from the table that the developed device has been experimentally verified for 20dB reflection reduction bandwidth as compared to [22], where measurement is reported only for 10dB reflection reduction and provides better reflection reduction value as compared to [21] and [23]. Compared with the lumped resistor based Metasurface absorbers, it provides better reflection reduction value as compared to [17] and [18] and wider 20dB reflection reduction as compared to [19]. In addition, the developed Metasurfaces have been analyzed for RCS reduction on planar, cylindrically bent and 90° dihedral surface which is not reported in previous

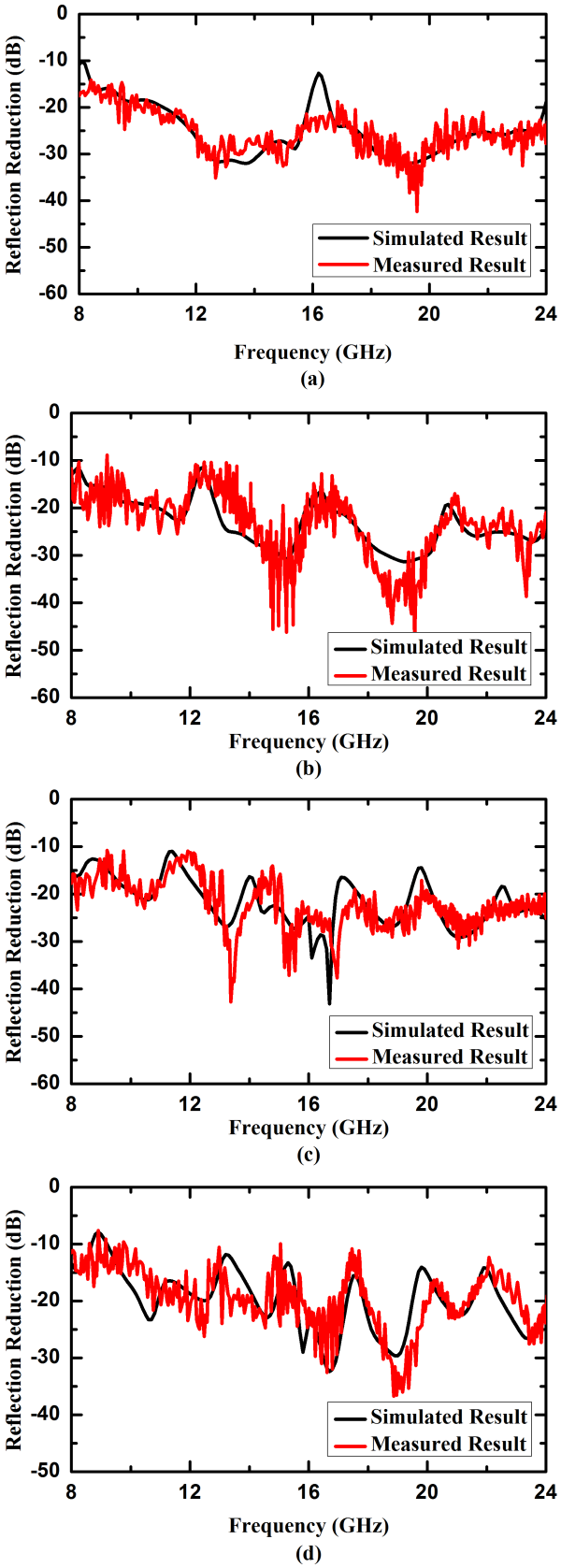

FIGURE 15. The simulated and measured reflection reduction for cylindrically bent Metasurface with radius of curvature 200mm with transmitter antenna fixed at 0° and receiver antenna kept at (a) 10° (b) 20° (c) 30° and (d) 40° with respect to normal to surface.

TABLE 1. Comparative performance of the developed device with previous reported work.

Ref.	Type	Unit cell Dimension	Thickness	Reflection Reduction Bandwidth	RCS Reduction	Polarization insensitivity
[17]	Lumped Element	13.6mm X 13.6mm	$0.077\lambda_L$	70.07% (5.3-11.2 GHz) (10dB)	Not reported	Yes
[18]	Lumped Element	15.5mm X 15.5mm	$0.082\lambda_L$	51.16% (8.2-13.4 GHz) (10dB)	Not reported	Yes
[19]	Lumped Element	11mm X10 mm	$0.120\lambda_L$	40% (8-12 GHz) (20dB)	Not Reported	No
[20]	Lumped Element	24.3mm X 24.3mm	$0.088\lambda_L$	126.8% (2-9 GHz) (10dB) and 83.4% (20dB)*	Not Reported	Yes
[21]	Resistive ink	24mm X 24mm	$0.08\lambda_L$	120% (3-12 GHz)(10dB)	Planar surface	Yes
[22]	Resistive ink	16mm X 16mm	$0.146\lambda_L$	68.69% (7.32 -14.98 GHz) (20dB)*	Not reported	Yes
[23]	Resistive ink	11mm X 11mm	$0.116\lambda_L$	96.29% (7-20 GHz) (15dB)	Not reported	Yes
This work	Resistive ink	11.8mm X 11.8mm	$0.120\lambda_L$	60% (10.5-19.5 GHz) (20dB)	Planar and Conformal surfaces	Yes

*Measurement reported only for 10dB reflection reduction.

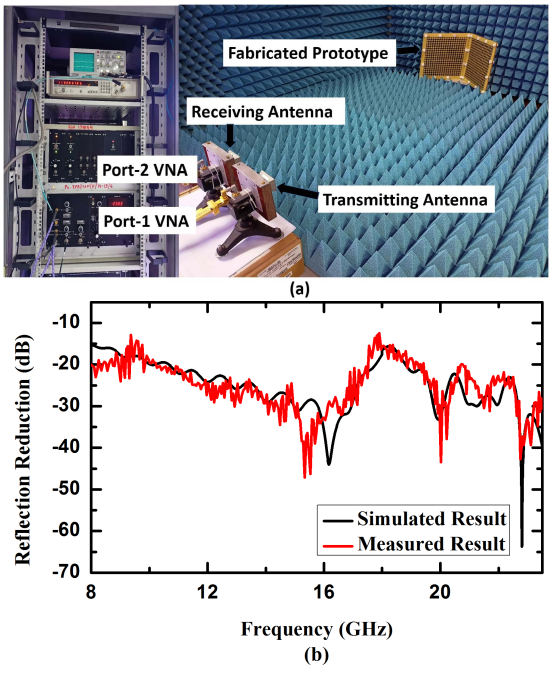

FIGURE 16. (a) Experimental setup and (b) The simulated and measured reflection reduction under normal incidence for 90° dihedral Metasurface.

works. This is our one of the major achievements. In another words, our study is innovative in terms of 20 dB reflection reduction as well as development and experimental validation of Conformal Metasurfaces for real time scenario RADAR application.

X. CONCLUSION

We have successfully designed, developed and experimentally characterized a resistive ink-based $0.12\lambda_L$ thick Metasurface absorber, in both planar and conformal configuration, and have achieved 20 dB reflection reduction for 60% FBW in frequency band 10.5-19.5 GHz under normal incidence and 10 dB reflection reduction under the oblique angle of incidence up to 40°. Further we have extensively analyzed the RCS reduction capability of the proposed absorber on planar, cylindrically bent and 90° dihedral surfaces and found that the proposed Metasurface absorber significantly reduces the RCS as compared to RCS of perfect electrical conductor (PEC) for both normal and oblique angles. From these observation, it is inferred that the proposed Metasurface absorber will find potential applications in radar stealth application as a standard absorbing device.

ACKNOWLEDGMENT

The simulations for the work reported in this article were performed on ANTYA, an IPR Linux Cluster.

REFERENCES

[1] E. F. Knott, M. T. Tuley, and J. F. Shaeffer, *Radar Cross Section*, 2nd ed. Raleigh, NC, USA: Scitech, 2004.

[2] K. J. Vinoy and R. M. Jha, *Radar Absorbing Materials: From Theory to Design and Characterization*, 1st ed. Norwell, MA, USA: Wolters Kluwer, 1996.
[3] W. W. Salisbury, "Absorbent body of electromagnetic waves," U.S. Patent 2 599 944, Jun. 10, 1952.
[4] R. L. Fante, M. T. McCormack, T. D. Syst, and M. A. Wilmington, "Reflection properties of the Salisbury screen," *IEEE Trans. Antennas Propag.*, vol. AP-36, no. 10, pp. 1443–1454, Oct. 1988.
[5] L. J. Du Toit, "The design of jauman absorbers," *IEEE Antennas Propag. Mag.*, vol. 36, no. 6, pp. 17–25, Dec. 1994.
[6] N. I. Landy, S. Sajuyigbe, J. J. Mock, D. R. Smith, and W. J. Padilla, "Perfect metamaterial absorber," *Phys. Rev. Lett.*, vol. 100, no. 20, May 2008, Art. no. 207402.
[7] S. B. Glybovski, S. A. Tretyakov, P. A. Belov, Y. S. Kivshar, and C. R. Simovski, "Metasurfaces: From microwaves to visible," *Phys. Rep.*, vol. 634, pp. 1–72, May 2016.
[8] D. R. Smith, W. J. Padilla, D. C. Vier, S. C. Nemat-Nasser, and S. Schultz, "Composite medium with simultaneously negative permeability and permittivity," *Phys. Rev. Lett.*, vol. 84, pp. 4184–4187, May 2000.
[9] N. Engheta and R. W. Ziolkowski, *Metamaterials: Physics and Engineering Explorations*, 1st ed. New York, NY, USA: Wiley, 2006.
[10] C. Caloz and T. Itoh, *Electromagnetic Metamaterials, Transmission Line Theory and Microwave Applications*, 1st ed. New York, NY, USA: Wiley, 2006.
[11] C. M. Watts, X. Liu, and W. J. Padilla, "Metamaterial electromagnetic wave absorbers," *Adv. Mater.*, vol. 24, no. 23, pp. OP98–OP120, Jun. 2012.
[12] S. Ghosh, S. Bhattacharyya, Y. Kaiprath, and K. V. Srivastava, "Bandwidth-enhanced polarization-insensitive microwave metamaterial absorber and its equivalent circuit model," *J. Appl. Phys.*, vol. 115, no. 10, Mar. 2014, Art. no. 104503.
[13] D. Kundu, A. Mohan, and A. Chakraborty, "Ultrathin polarization independent absorber with enhanced bandwidth by incorporating Giusepe peano fractal in square ring," *Microw. Opt. Technol. Lett.*, vol. 57, no. 5, pp. 1072–1078, May 2015.
[14] S. Ghosh, S. Bhattacharyya, and K. V. Srivastava, "Bandwidth-enhancement of an ultrathin polarization insensitive metamaterial absorber," *Microw. Opt. Technol. Lett.*, vol. 56, no. 2, pp. 350–355, 2014.
[15] S. Ghosh, S. Bhattacharyya, D. Chaurasiya, and K. V. Srivastava, "Polarisation-insensitive and wide-angle multi-layer metamaterial absorber with variable bandwidths," *Electron. Lett.*, vol. 51, no. 14, pp. 1050–1052, Sep. 2015.
[16] B. A. Munk, *Frequency Selective Surfaces: Theory and Design*. New York, NY, USA: Wiley, 2000.
[17] D. Kundu, A. Mohan, and A. Chakrabarty, "Single layer wideband microwave absorber using array of crossed dipoles," *IEEE Antennas Wireless Propag. Lett.*, vol. 15, pp. 1589–1592, 2016.
[18] T. T. Nguyen and S. Lim, "Design of metamaterial absorber using eight-resistive-arm cell for simultaneous broadband and wide-incidence-angle absorption," *Sci. Rep.*, vol. 8, no. 1, p. 6633, Dec. 2018.
[19] A. P. Sohrab and Z. Atlasbaf, "A circuit analog absorber with optimum thickness and response in X-band," *IEEE Antennas Wireless Propag. Lett.*, vol. 12, pp. 276–279, 2013.
[20] Y. Shang, Z. Shen, and S. Xiao, "On the design of single-layer circuit analog absorber using double-square-loop array," *IEEE Trans. Antennas Propag.*, vol. 61, no. 12, pp. 6022–6029, Dec. 2013.
[21] D. Kundu, S. Baghel, A. Mohan, and A. Chakrabarty, "Design and analysis of printed lossy capacitive surface-based ultrawideband low-profile absorber," *IEEE Trans. Antennas Propag.*, vol. 67, no. 5, pp. 3533–3538, May 2019.
[22] M. Olszewska-Placha, B. Salski, D. Janczak, P. R. Bajurko, W. Gwarek, and M. Jakubowska, "A broadband absorber with a resistive pattern made of ink with graphene nano-platelets," *IEEE Trans. Antennas Propag.*, vol. 63, no. 2, pp. 565–572, Nov. 2014.
[23] F. Costa, A. Monorchio, and G. Manara, "Analysis and design of ultra thin electromagnetic absorbers comprising resistively loaded high impedance surfaces," *IEEE Trans. Antennas Propag.*, vol. 58, no. 5, pp. 1551–1558, May 2010.
[24] C. A. Balanis, *Advanced Engineering Electromagnetics*. Hoboken, NJ, USA: Wiley, 1989.
[25] W. Chen, C. A. Balanis, and C. R. Birtcher, "Checkerboard EBG surfaces for wideband radar cross section reduction," *IEEE Trans. Antennas Propag.*, vol. 63, no. 6, pp. 2636–2645, Jun. 2015.
[26] A. Y. Modi, C. A. Balanis, C. R. Birtcher, and H. N. Shaman, "Novel design of ultrabroadband radar cross section reduction surfaces using artificial magnetic conductors," *IEEE Trans. Antennas Propag.*, vol. 65, no. 10, pp. 5406–5417, Oct. 2017.
[27] P. Tiwari, S. K. Pathak, V. P. Anitha, V. Siju, and A. Sinha, "X-band Γ-shaped anisotropic metasurface-based perfect cross-polarizer for RCS reduction," *J. Electromagn. Waves Appl.*, vol. 34, no. 7, pp. 894–906, May 2020.
[28] P. Tiwari, S. K. Pathak, and V. P. Anitha, "Design, development and characterization of wide incidence angle and polarization insensitive metasurface absorber based on resistive-ink for X and Ku band RCS reduction," *Waves Random Complex Media*, Sep. 2021, doi: 10.1080/17455030.2021.1972182.
[29] *Y-Shield EMR Protection*. Accessed: Sep. 3, 2020. [Online]. Available: https://www.yshield.com/
[30] *Siddhi Vinayaka Graphics Pvt Ltd*. Ahmedabad, Gujarat. Accessed: Dec. 9, 2020. [Online]. Available: https://siddhi-vinayaka-graphics-pvt-ltd.business.site/

PRIYANKA TIWARI (Student Member, IEEE) received the B.E. degree in electronics and telecommunications from the Institute of Engineering and Technology (IET), DAVV, Indore, India, in 2011, and the M.Tech. degree in electronics and communications from the Malaviya National Institute of Technology (MNIT), Jaipur, India, in 2013. She is currently pursuing the Ph.D. degree with the Institute for Plasma Research, Gandhinagar, under the aegis of Homi Bhabha National Institute (HBNI), Mumbai, India. From 2013 to 2015, she was an Associate System Engineer at IBM India Pvt. Ltd., Pune, India. Her research interests include design and realization of Metasurface based devices for radar stealth application.

SURYA KUMAR PATHAK (Senior Member, IEEE) received the Ph.D. degree in electromagnetics and microwave engineering from the Department of Electronics and Communication Engineering, IIT BHU, Varanasi, India. He joined as an Engineering Faculty Member with the Institute for Plasma Research, Gandhinagar, Gujarat, where his studies mainly evolved around teaching of electromagnetics of plasma and doing microwave engineering instrumentations and developments. He has successfully developed the Millimeter Wave Laboratory and various measurement devices and systems, such as interferometers, reflectometer, radiometer, and fast scan Fourier-transform interferometer systems from microwave to THz spectrum. He is actively involved in teaching as well as academics programs, where he does research on EM wave propagation in bio-media, plasma and metamaterials, microwave and optical waveguides, and antenna engineering. He has published more than 75 articles in various international journals and holds one U.S. patent. He is a Senior Member of IEEE Antenna and Propagation Society.

VARSHA SIJU received the M.Sc. degree in applied physics from Annamalai University, Annamalainagar, India, in 2008. She is currently pursuing the Ph.D. degree in plasma physics. She joined as a Diagnostician with the Institute for Plasma Research, Gandhinagar, India, in 2004. Since 2004, she has been working on the design, development, and characterization of various microwave plasma diagnostics, like interferometer, reflectometer, and radiometer. Her research interests include design and development of receiver systems that can used for societal benefits, exploring applications in the mmwave spectrum, understanding the electromagnetic wave propagation in plasma and other dielectric media, experimental characterization of different materials used for different microwave applications, and antenna measurements. She is a Lifetime Member of the Plasma Science Society of India.